Neural Networks 24 (2011) 333–344

Contents lists available at ScienceDirect

Neural Networks

journal homepage: www.elsevier.com/locate/neunet

A model study on the circuit mechanism underlying decision-making in *Drosophila*

Zhihua Wu [a,*], Aike Guo [a,b,1]

[a] State Key Laboratory of Brain and Cognitive Science, Institute of Biophysics, Chinese Academy of Sciences (CAS), 15 Datun Road, Chaoyang District, Beijing 100101, China
[b] Institute of Neuroscience, State Key Laboratory of Neuroscience, Shanghai Institutes for Biological Sciences, CAS, 320 Yueyang Road, Shanghai 200031, China

ARTICLE INFO

Article history:
Received 24 May 2010
Received in revised form 27 October 2010
Accepted 17 January 2011

Keywords:
Systems-level circuit model
Drosophila
Decision-making
Dopamine modulation
Attention
Feature binding

ABSTRACT

Previous elegant experiments in a flight simulator showed that conditioned *Drosophila* is able to make a clear-cut decision to avoid potential danger. When confronted with conflicting visual cues, the relative saliency of two competing cues is found to be a sensory ruler for flies to judge which cue should be used for decision-making. Further genetic manipulations and immunohistological analysis revealed that the dopamine system and mushroom bodies are indispensable for such a clear-cut or nonlinear decision. The neural circuit mechanism, however, is far from being clear. In this paper, we adopt a computational modeling approach to investigate how different brain areas and the dopamine system work together to drive a fly to make a decision. By developing a systems-level neural network, a two-pathway circuit is proposed. Besides a direct pathway from a feature binding area to the motor center, another connects two areas via the mushroom body, a target of dopamine release. A raised dopamine level is hypothesized to be induced by complex choice tasks and to enhance lateral inhibition and steepen the units' response gain in the mushroom body. Simulations show that training helps to assign values to formerly neutral features. For a circuit model with a blocked mushroom body, the direct pathway passes all alternatives to the motor center without changing original values, giving rise to a simple choice characterized by a linear choice curve. With respect to an intact circuit, enhanced lateral inhibition dependent on dopamine critically promotes competition between alternatives, turning the linear- into nonlinear choice behavior. Results account well for experimental data, supporting the reasonableness of model working hypotheses. Several testable predictions are made for future studies.

1. Introduction

Decision-making is a capability crucial for the animals' existence. In everyday life humans and animals need to make decision almost all the time on things ranging from food taste to political opinion. The fruit fly *Drosophila melanogaster*, without exception, is able to make a decision. Examples range from simple selections in females toward egg-laying sites (Yang, Belawat, Hafen, Jan, & Jan, 2008) to saliency-based decision-making when confronted with conflicting cues in a flight simulator (Tang & Guo, 2001; Zhang, Guo, Peng, Xi, & Guo, 2007). The latter occurs only among flies experienced in prior training, during which they learned to turn aside from a certain visual pattern to avoid heat punishment. Facing an upper-blue bar, for instance, is always accompanied with heat punishment, whereas it is safe if flight directions are towards a lower-green bar. Conditioned flies prefer the lower-green bar even if the heat punishment is shut down, showing that an association memory is established. To find out whether the flies have the ability to make a choice, a new paradigm different from classic memory tasks was developed, in which flies were confronted with conflicting cues (Tang & Guo, 2001; Zhang et al., 2007). The paradigm presents to flies a pair of bars with their colors exchanged and vertical separation decreased compared with that used for training (Zhang et al., 2007). And heat punishment is removed. The vertical separation between the bars' centers of gravity quantifies the position saliency of the two bars and is denoted as ΔCOG. In such a design safety and danger cues are mixed together. Which bar should be followed to avoid potential danger? Apparently a good memory alone is not enough to resolve the dilemma. Something like "intelligence" is urgently needed.

Surprisingly wild-type *Drosophila* can make a clear-cut decision by taking a salience-based strategy (Guo, Zhang, Peng, & Xi, 2009, 2010; Tang & Guo, 2001; Zhang et al., 2007). Specifically, if ΔCOG is close to 60° as learned, flies rapidly turn towards the lower-blue bar (Zhang et al., 2007). It is a choice according to the saliency of position but not color cue. Otherwise, if ΔCOG is close to 0°, color is

* Corresponding author. Tel.: +86 010 64869355.
E-mail addresses: wuzh@moon.ibp.ac.cn (Z. Wu), akguo@ion.ac.cn (A. Guo).
[1] Tel.: +86 021 54921785.

0893-6080/$ – see front matter © 2011 Elsevier Ltd. All rights reserved.
doi:10.1016/j.neunet.2011.01.002

treated as a cue much more salient than position. Flies select to face the upper-green bar. A sigmoid regression curve was found to fit the function between ΔCOG and choice preference index (PI) very well, which defines a choice curve. This clear-cut decision behavior is called nonlinear choice.

Taking advantage of a genetically tractable system, it was further revealed that flies with a defective mushroom body (MB) or with dopaminergic projection to the MB blocked show a linear but not nonlinear choice behavior (Tang & Guo, 2001; Zhang et al., 2007). A linear choice means that the choice PI is linearly proportional to ΔCOG if the task is repeated with a varied ΔCOG in the range (0°, 60°). The PI measures the difference in the percentage of time spent following the position or color cue. Nonlinear choice is characterized by a rapid clear-cut decision, and flies seldom turn back towards the non-selective target once a decision is made. By contrast, PIs are substantially reduced in the simple linear choice, in which flies seem hesitant and have difficulty in deciding which bar to follow. Data show that the dopamine-MB circuit is not necessary for linear choice but remarkably involved in nonlinear choice (Zhang et al., 2007).

The result is nontrivial if we notice the similarities in decision-making between primates and *Drosophila*. Dopamine is an important neurotransmitter or neuromodulator for both mammals and insects. In higher mammals the midbrain dopaminergic system contributes to value-based decisions, at least through its role in reward valuation and prediction (Montague, Hyman, & Cohen, 2004; Rangel, Camerer, & Montague, 2008; Sugrue, Corrado, & Newsome, 2005). In the regulation of behavioral activity, the MB is similar to the prefrontal cortex to some extent (Heisenberg, 2003). The prefrontal and parietal association cortices, for instance, are the location for decision making by linking rewards to behavioral responses (Kepecs, Uchida, Zariwala, & Mainen, 2008; Sugrue et al., 2005), and a comparable role might be played by the MB in *Drosophila* (Tang & Guo, 2001; Zhang et al., 2007). The comparison prompts us to think that the neural mechanism underlying decision-making might be highly conserved from insects to primates. Elucidating how a decision emerges in flies, whose neural circuit is much simpler than that of primates, is undoubtedly helpful in understanding the general choice mechanism.

However, it is so far difficult to address the problem by conventional methods such as electrophysiological recordings, although quite a few studies have now recorded single cells (Turner, Bazhenov, & Laurent, 2008) or a local field potential (Nitz, van Swinderen, Tononi, & Greenspan, 2002) in *Drosophila*. The limitation is in sharp contrast to the virtues of *Drosophila* as a model for systems neuroscience. In this study we adopt a network modeling approach to simulate the decision-making circuit. By constructing a systems-level network model with multiple modules, the neurocomputational mechanisms underlying an experience-dependent formation of value, the modulation role of dopamine in the transformation between linear and nonlinear decisions, and etc. are elucidated. Computer simulations account for data observed by Zhang et al. (2007), and the model makes several testable predictions for future experimental studies.

2. Methods

2.1. Anatomical organization of decision-making circuit

While identifying brain areas involved in making a decision is a big challenge, new tools for detecting neural activity in the fly have been greatly developed recently (Olsen & Wilson, 2008). By gathering and organizing relevant data below, we argue for a multiple-module circuit. It consists of structures that specifically serve feature detecting, feature binding, danger detecting, and decision-making, respectively (Fig. 1(A)). Note that

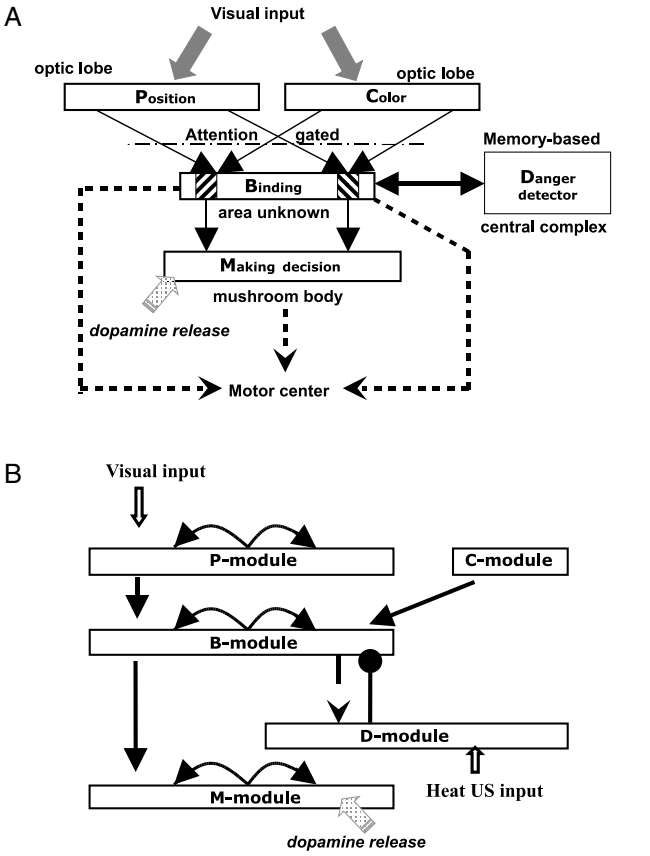

Fig. 1. Network model for decision-making task in *Drosophila*. (A) Schematic model architecture. Input to binding module is gated by attention (dot–dashed line). Hatched boxes mark two recognized visual bars with different colors in the binding area. The MB is the only target of dopamine release (filled arrow). The transformation from a decision to an action (dashed lines) is not simulated. (B) Multiple-module network extracted from (A). From *B*- to *D*-module the feed-forward projection is plastic (broken arrow) and the feedback connection is inhibitory (solid circle).

the transformation of a decision into a motor center is not considered here.

As a first step of visual information processing, five pattern features including color, size, and vertical position or elevation in the panorama can be recognized in *Drosophila* (Dill & Heisenberg, 1995; Ernst & Heisenberg, 1999; Tang, Wolf, Xu, & Heisenberg, 2004). A number of classes of neurons respond specifically to small moving targets in the third optic ganglion of several species of flies (Egelhaaf, 1985; Gilbert & Strausfeld, 1992; Nordstrom, Barnett, & O'Carroll, 2006). With respect to color processing, two types of columnar neurons downstream of the chromatic channels R7 and R8 are recently identified in the medulla in *Drosophila*, which could function as color opponent cells (Gao et al., 2008). These evidences support that the optic lobe or the visual periphery houses position and color detectors, as labeled in the top of Fig. 1(A), though their exact anatomical location remains unknown.

Flies recognize a composite pattern as a whole by combining multiple features (Tang et al., 2004). Feature binding was proposed to occur in a sensory-motor center of the central brain (Tang et al., 2004), though the circuit connecting feature detectors with the higher visual center is largely unclear so far. In our model the module for feature binding is labeled as 'area unknown' to keep objectivity (Fig. 1(A)). It should be noted that although a previous artificial network proposed a robust function of the MB on visual recognition in insects (Huerta & Nowotny, 2009), no direct projection from optical lobes to the MB is found in *Drosophila* yet. In fact flies without MBs are quite normal in visual and motor

learning (Heisenberg, 2003), which evidences that the feature binding module cannot be replaced by the MB.

Feature binding area in the model is hypothesized to be the first place for forming a simple decision, where the competition among potential choices is biased by visual memory. Associative memory is established during training by linking a particular set of values of position and color to heat punishment. Considering that short-term memory for position feature is stored in the fan-shaped body (Liu et al., 2006), our model tentatively assumes that the anatomical substrate for memory-based biasing or danger detecting corresponds to the central complex (Fig. 1(A)). By 'tentatively' it means that we indeed note that the exact location of color memory is unclear as yet.

A key point of the model lies in whether the simple choice is fed forwards to the motor center by one pathway or not. The toolset offered by *Drosophila* genetic revealed two distinct pathways in all probability (Zhang et al., 2007). In flies with disrupted MB or blocked dopaminergic projections to the MB a clear-cut choice is impossible, but a linear choice behavior remains. The data indicate that the MB is not needed for simple linear choice (Zhang et al., 2007). Sparked by these evidences, our model argues for a two-pathway circuit from binding area to motor center, as shown in Fig. 1(A). The direct pathway is a default setting, while the second one via the MB is activated only when confronted with complex tasks. There are eight different morphological classes of dopamine neurons innervating the MB in *Drosophila* (Mao & Davis, 2009). The second pathway via the MB should be seriously modulated by dopamine.

2.2. Working hypotheses

We propose the following hypotheses on the circuit model for decision-making in *Drosophila*:

(1) Visual selective attention controls what specific cues enter the feature binding area at a particular moment.
(2) There is a topographic spatial map connecting five modules of the circuit. The application of an unconditioned stimulus (US) of heat punishment is also topographic.
(3) A decision is first formed in the binding area, where the choice process is strongly biased by feature-dependent memory. It underlies the simple decision behavior characterized by a linear choice curve.
(4) The circuit features two pathways from the binding area to the motor center. One is direct way as a default setting, while another passes through the MB and is switched on only when a complex task calls.
(5) In the face of a complex choice task, the ambiguous/conflicting visual cues elicit a phasic response of dopaminergic neurons projecting to the MB, resulting in a transient increase in dopamine levels in the MB.
(6) Phasic dopamine modulates the neuronal dynamics of the MB, leading to a rapid amplification of the slight difference between two potential choices. It makes the one with a slightly stronger value win the competition finally.

Selective attention was proposed for *Drosophila* visual orientation (Heisenberg & Wolf, 1984). Attention-like fixation or tracking behavior induced by visual targets at a flight simulator was reported in fruit flies (Heisenberg, Wolf, & Brembs, 2001; van Swinderen, 2005; Wu, Gong, Feng, & Guo, 2000). These studies underlie hypothesis (1). As is well known, there is a topographic map of odor quality in the antennal lobe in the *Drosophila* brain. The motion-sensitive large-field neurons in the lobula plate have distinct receptive fields that are orderly mapped (Joesch, Plett, Borst, & Reiff, 2008), showing a topographic spatial map for visual motion detection in the optic lobe of *Drosophila*. Hypothesis (2) is based on such findings, although it is still unclear whether neighboring points in a visual image evoke activity in neighboring neurons of central brain areas like the MB. In this manner, the model circuit maintains the information of spatial locations of stimuli.

The reasonableness of hypotheses (3) and (4) has been defended by reviewing relevant evidences in Section 2.1. Hypotheses (5) and (6) suggest a critical role of the dopaminergic-MB circuit in the competition between two potential choices. While the involvement of this circuit in nonlinear decision-making is supported by Tang and Guo (2001) and Zhang et al. (2007), we need to discuss how a modulation role of dopamine is achieved.

Eight different morphological classes of dopamine neurons innervate the MB in *Drosophila*, and most of which project to the MB lobes (Mao & Davis, 2009). To our knowledge, there is to date no report about how the dopamine concentration in the MB is modulated by a conditioned stimulus (CS). The most relevant study showed that when CS odor is presented after aversive conditioning, the duration of the activities of dopaminergic neurons is prolonged, suggesting a US-predicting role of dopaminergic neurons (Riemensperger, Voeller, Stock, Buchner, & Fiala, 2005).

In mammals, midbrain dopaminergic neurons exhibit phasic responses to a wide type of unexpected biologically significant events including sudden novel stimuli, intense sensory stimuli, motivating stimuli, primary rewards and arbitrary stimuli similar to those classically conditioned by association with primary rewards (Redgrave & Gurney, 2006; Schultz, 2007). Such responses show short latency (70–100 ms) and short duration (<200 ms). Moreover dopaminergic neurons show a sustained increase in activity that grows from the onset of the reward uncertainty-predicting stimulus (Fiorillo, Tobler, & Schultz, 2003). Considering that the dopamine function in predicting a reinforcing stimulus is partially conserved in insects (Riemensperger et al., 2005), we propose in hypothesis (5) that dopaminergic neurons may also show increased response to reinforcer uncertainty in *Drosophila*. In Zhang et al. (2007) reinforcer uncertainty is generated due to a mixing of visual cues predicting punishment and safety respectively. To flies, the conflicting cues could mean anything: totally novel stimuli different from the learned one or punishment reinforcer uncertainty. Such conflicting cues could induce an increase in dopaminergic neurons' activities and subsequently result in elevated dopamine levels in the MB, according to hypothesis (5).

Hypothesis (6) proposes a computational role of dopamine in the target MB. It is unclear yet whether dopaminergic neurons communicate by volume transmission (Fuxe et al., 2009) or only by localized activity of specific synapses in *Drosophila*. And currently little is known about the functional properties of dopamine receptors in the *Drosophila* central nervous system. However, both D1 and D2 dopamine receptors together with receptor targets are well-conserved in *Drosophila* and especially highly enriched in the MB neuropil (Han, Millar, Grotewiel, & Davis, 1996; Hearn et al., 2002; Kim, Lee, Seong, & Han, 2003). We thus base hypothesis (6) on the better known properties of dopamine modulation in some mammals (Cohen, Braver, & Brown, 2002; Nicola, Surmeier, & Malenka, 2000). The specific dopamine modulation on MB cells is described in detail in Section 2.4.4.

2.3. Overall network architecture

We try to develop a minimal network model at a systems-level required to account for decision-making in *Drosophila*. This network is not intended to simulate neural activity at a neurophysiological level or to capture data on individual fly brain areas, cell types, but it aims at explaining and predicting the systems and behavioral level phenomena. The mathematical equations used significantly simplify the operations that may actually take place in the nervous system.

The whole network consists of five modules (Fig. 1(B)), responsible for position feature detecting (*P*-module), color feature detecting (*C*-module), feature binding (*B*-module), danger detecting (*D*-module), and decision-making (*M*-module), respectively. Note the transformation of neural activities into motor commands is omitted in the model. All modules comprise N neuron units arranged in a line except the *C*-module that includes two units encoding blue and green color, respectively, for simplification. The connections between modules are hardwired and feed-forward except that between *B*- and *D*-modules. The *D*-module detects danger by receiving heat punishment US. The connection weights from *B*- to *D*-modules are endowed with synaptic plasticity during training, although it is currently unclear where the visual CS and heat US actually meet in the insect brain. *D*-module consists of inhibitory units, which have a faster time constant than those of other modules. It gives a rapid inhibitory feedback to the unit group in *B*-module encoding the visual bar with conditioned danger feature.

The dynamics of individual units are governed by a firing rate model as follows:

$$\tau^{Mo}\frac{\mathrm{d}V_i^{Mo}}{\mathrm{d}t} = -V_i^{Mo} + E_i^{Mo} - I_i^{Mo} + \Theta(0,\eta), \tag{1}$$

where V_i^{Mo} is the activity of the ith unit of a given module Mo and τ^{Mo} is the time constant. The module superscript Mo will be replaced below by P, C, B, D, and M for each specific module, respectively. E^{Mo} and I^{Mo} are the excitatory and inhibitory input, respectively. $\Theta(0,\eta)$ is Gaussian noise with mean 0 and variance η, modeling background fluctuations. The output firing rate of units is a logistic sigmoid function $r_i^{Mo} = 1/(1+\mathrm{e}^{(1-V_i^{Mo})/\beta})$ with parameter β regulating the slope. Although the dynamics of specific neurons in the fly brain is unknown, the employment of Eq. (1) in our systems-level model is reasonable because it captures the general properties of neuron firing.

Except the *C*- and *D*-modules explained below, the recurrent or lateral connections within a module are defined as a Difference-of-Gaussians function:

$$\begin{aligned} W_d &= \kappa\cdot(\mathrm{e}^{-d^2/32} - 0.4\mathrm{e}^{-d^2/128}) - \rho \\ WE_{ij} &= [W_{(i-j)}]^+ \\ WI_{ij} &= [-\alpha\cdot W_{(i-j)}]^+ \end{aligned} \tag{2}$$

where $[x]^+$ is defined as $\max(x,0)$. WE_{ij} and WI_{ij} are the excitatory and inhibitory kernels, respectively, representing the lateral connections from the jth to ith unit. Parameter α controls the strength of lateral inhibition. According to model hypothesis, a topographic spatial map exists among modules. Neighboring cell units have partially overlapping receptive fields in each module, and units are arranged by their preferred position of visual targets. The nature of interaction described in (2) is based on data about lateral connections among neighboring units with similar or different preferred stimuli, which is widely used in recurrent network modeling (Cisek, 2006; Dayan & Abbott, 2001). Specifically, lateral connections are characterized by an on-center-off-surround architecture as shown in Fig. 2(A), where interactions vanish for units too far away from each other.

Parameters are set as $N = 80$, $\eta = 0.5$, $\tau^{Mo} = 20$ ms except $\tau^C = 30$ ms and $\tau^D = 5$ ms, and $\kappa = 1.0$, $\rho = 0.1$ with an exception $\rho = 0.01$ in the *P*-module. Except where otherwise indicated, we use $\beta = 0.3$ for the sigmoid function of unit output and $\alpha = 1.0$ for the lateral inhibition strength. The integration time step is 0.02 ms. Different time constants are based on biological realism in mammals. Inhibitory neurons have much shorter membrane time constants than excitatory neurons do, which is widely used in models (Gruber, Dayan, Gutkin, & Solla, 2006; Wang, 2002). The brain area involved in color processing has a slower dynamics relative to other visual areas, as modeled in Cisek (2006). A smaller value of parameter ρ in *P*-module leads to much stronger excitatory and weaker inhibitory recurrent connections. This setting comes from the functional consideration of helping to form a noise against encoding of position features, even with a weak input.

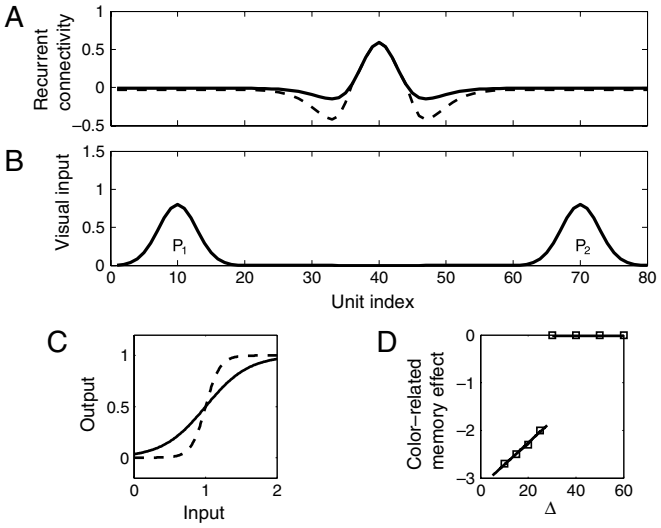

Fig. 2. Network characteristics. (A) Lateral synaptic connections within *P*-, *B*-, and *M*-modules. Neighboring units with similar (different) preferred stimuli excite (inhibit) one another, while interactions vanish for units too far away from each other (solid curve with $\alpha = 1.0$). Lateral inhibition can be enhanced in the *M*-module by an elevated dopamine level (dashed curve with $\alpha = 2.8$). (B) Two bumps of activity induced in *P*-module by visual input of two bars. Center units with index P_1 and P_2 show a preferred response to the position of two bars, respectively. (C) The sigmoid output function of units (solid curve with $\beta = 0.3$) is steepened within *M*-module by elevated dopamine level (dashed curve with $\beta = 0.1$). (D) Inhibition effect $f^C(\Delta)$ of color-related memory on *B*-module as a function of the saliency of position feature.

The dependence of the model on small changes in all parameters including those defined in the following subsections is analyzed by varying each parameter to either increase or decrease in each simulation run. Amounts of simulations performed show that the model is robust to precise fine-tuning of each parameter, and our results are insensitive to the specific choice of parameter values.

2.4. Details of individual modules

2.4.1. Visual input and feature detector modules

Two pairs of visual horizontal bars used in behavior experiments in Zhang et al. (2007) are reduced to one pair in the model for simplification (Fig. 3(A)). Due to a large visual field of about 270° in *Drosophila*, two bars should always be visible. This is simulated by a persistent input to *P*- and *C*-modules. *P*-module houses position detector units with a resolution of 1°. Units have preferred vertical positions uniformly covering the interval $[-(N/2)^\circ, +(N/2)^\circ] = [-40^\circ, +40^\circ]$. These units have Gaussian receptive fields, resulting in two bumps of activity in *P*-module. The spatial distance $\Delta = P_2 - P_1$ between two bumps thus encodes the physical separation ΔCOG between two bars, where P_1 and P_2 denote the unit index of two bump centers showing maximal activity (Fig. 2(B)). For the sake of clarity, the locations of units P_1 and P_2 are always symmetric to the center of the *P*-module. Instead of the ΔCOG, parameter Δ below describes the position saliency of visual targets.

The total excitatory and inhibitory inputs to the ith unit of *P*-module are as follows:

$$\begin{aligned} E_i^P &= \sum_j WE_{ij}\cdot r_j^P + \mathrm{VI}_i^P \\ I_i^P &= \sum_j WI_{ij}\cdot r_j^P \end{aligned} \tag{3}$$

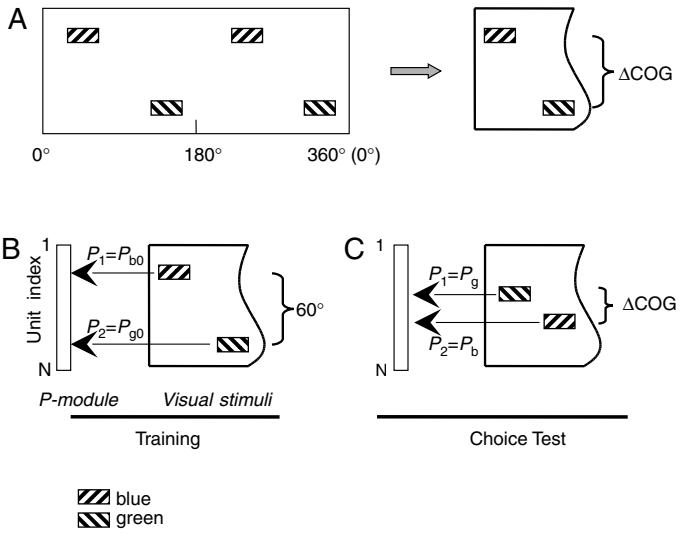

Fig. 3. Task scheme for computer simulations. (A) Visual input of four bars in behavior experiments in the flight simulator is reduced to one pair of bars in the model. (B) Training task. Two bars with $\Delta\mathrm{COG} = 60^\circ$ (right) are presented to the P-module consisting of N units (left), which induce two bumps of activities at P_1 and P_2, respectively. (C) Choice task in which both the color and bar separation are changed compared with training.

$$\mathrm{VI}_i^P = 0.8\left(\mathrm{e}^{-\frac{(i-P_1)^2}{2\sigma^2}} + \mathrm{e}^{-\frac{(i-P_2)^2}{2\sigma^2}}\right)$$

where VI_i^P is the visual input, and σ controls the width of the Gaussian receptive field of individual units ($\sigma = 4.0$).

For the sake of clarity, only two color detector units are included in the C-module with preferred colors blue and green respectively. There are no recurrent connections within this module. The excitation and inhibition inputs to the ith unit are defined as:

$$E_k^C = \mathrm{VI}_k^C = 1.5$$
$$I_k^C = 0.1 r_{k'}^C \quad (k \neq k') \tag{4}$$

where k or $k' = \{1, 2\}$, and VI_k^C takes the same value for both green and blue, simulating the color input.

2.4.2. Feature binding module

The binding module receives input from P- and C-modules to help object perception and recognition (Treisman, 1998). According to hypothesis (3), it also functions as the location for simple decisions to be made under memory-dependent biasing.

Let us first focus on the input from feature detector modules, which is hypothesized to be controlled by the shift of the attention window. Features cannot be reported to the B-module unless the feature occurs in the window of attention. It is consistent with a working model of translation invariance (Tang et al., 2004). For naïve flies, it is reasonable to assume that the window of attention randomly spotlights visual targets with equal probability. It accords with a crucial property of attentional deployment: the process by which the currently attended location is prevented from being attended again (Itti & Koch, 2001). With respect to conditioned flies, top–down control may affect attention on the basis of bottom–up cues. In the model, however, the shifting pattern of the attention window is assumed to be independent of experience for simplification. Actually in face of two bars having cues, predicting safety and danger, mixed together, adopting a random shifting of attention spotlight is natural or reasonable to animals.

By defining parameter ATN_i to simulate the effect of the attention window, the B-module has the following inputs:

$$E_i^B = \sum_j WE_{ij} \cdot r_j^B + \mathrm{ATN}_i \cdot (w_{ii}^{P\to B} \cdot r_i^P + w_{ik}^{C\to B} \cdot r_k^C)$$
$$I_i^B = \sum_j WI_{ij} \cdot r_j^B + w_{ii}^{D\to B} \cdot r_i^D + f^C(\Delta) \tag{5}$$

where $w_{ij}^{P\to B}$ is synaptic weight from the jth unit of the P-module to the ith one of the B-module ($w_{ij}^{P\to B} = 2.5$ for $j = i$ and falls off to zero otherwise). The C-module projects to the B-module with a low spatial resolution. The specific weight is $w_{ik}^{C\to B} = 2.0$ for $|i - P_k| < 10$ ($k = 1$ or 2) and otherwise falls off to zero. The attention window randomly spotlights two bars with a period of 100 ms and covers one bar each time. Since the P-module only holds two bumps, parameter ATN_i simply takes 0 or 1 with probability 0.5 at the beginning of every 100 ms period, where $i = 1, \ldots, N/2$ and $\mathrm{ATN}_{i+40} = 1 - \mathrm{ATN}_i$.

The last two terms in the second formula of Eq. (5) describe a biasing modulation due to danger-related memory. Position memory is stored in $w_{ij}^{B\to D}$ as explained in the next Subsection, while feedback connections from D- to B-modules have no plasticity for simplification ($w_{ij}^{D\to B} = 5.0$ for $j = i$ and falls off to zero otherwise). Color-related learning and memory is not explicitly simulated in the model for simplification. But its effect is mimicked by the function $f^C(\Delta)$, which will be explained in detail in the section "Results" below.

2.4.3. Danger detecting module

As the site of position memory storage, the D-module can be activated by input from the B-module through learned synaptic connections $w_{ij}^{B\to D}$ after conditioning and/or by heat US stimulus during conditioning.

An association between heat punishment and position feature is established during conditioning. No lateral connections are proposed in the D-module to emphasize the US, and the excitatory and inhibitory inputs are as follows:

$$E_i^D = \mathrm{US}_i + w_{ii}^{B\to D} \cdot r_i^B$$
$$I_i^D = 0.0 \tag{6}$$

where US_i describes heat US-induced input with value 1.0 for $|i - P| < 10$ and 0 otherwise. Here P denotes the center unit index of the group encoding the bar coupled with heat punishment during conditioning. Synaptic weight $w_{ii}^{B\to D}$ has initial values 0 before training and obeys the following learning rule. Note $w_{ij}^{B\to D}$ is zero for $j \neq i$.

$$\tau^{\mathrm{Learning}} \frac{\mathrm{d}w_{ii}^{B\to D}}{\mathrm{d}t} = r_i^B \cdot r_i^D - 0.1(r_i^D)^2 \cdot w_{ii}^{B\to D} \tag{7}$$

where τ^{Learning} is a time constant controlling the learning rate. This is a typical Oja rule with a good stability and widely used

in network modeling (Dayan & Abbott, 2001). The evidence for Hebbian plasticity learning rule in insects was recently reported (Cassenaer & Laurent, 2007).

2.4.4. Decision-making module

When confronted with conflicting cues, the M-module is switched on to help solve the choice problem according to model's hypotheses. Compared with other modules, the M-module is the sole target of dopaminergic release. A raised dopamine level in the M-module is hypothesized to enhance the lateral inhibition between units (Fig. 2(A)) and steepen individual units' response function (Fig. 2(C)). The M-module units have the following inputs:

$$E_i^M = \sum_j WE_{ij} \cdot r_j^M + w_{ii}^{B\to M} \cdot r_i^B$$
$$I_i^M = \sum_j WI_{ij} \cdot r_j^M \tag{8}$$

where the last term of the first formula represents the direct projection from the B-module, here $w_{ij}^{B\to M} = 2.5$ for $j = i$ and falls off to zero otherwise. Dopamine modulation takes effect by resetting the values of parameters β in r_j^M and α in WI_{ij} of the M-module. Two examples are shown by the dashed curve in Fig. 2(A) and (C) respectively, where the lateral inhibition and unit response gain are separately increased by 2.8 and 3 times.

The computational role of dopamine assumed above is based on the better-known modulation of dopamine in some mammals. Gain control in Fig. 2(C) describes the catecholamine-, particularly dopamine-mediated increases in the responsibility or signal-to-noise ratio of cortical neurons (Gruber et al., 2006; Servan-Schreiber, Printz, & Cohen, 1990), which is generally consistent with the stabilization effects of dopamine in biophysically-grounded cortical models (Brunel & Wang, 2001; Durstewitz, Seamans, & Sejnowski, 2000). The enhanced lateral inhibition, as shown in Fig. 2(A), is indirectly defended by several evidences. The D1 dopamine receptor increases the excitability of fast-spiking interneurons, which enhances evoked and spontaneous IPSCs recorded in pyramidal cells in the prefrontal cortex (Gorelova, Seamans, & Yang, 2002; Seamans, Gorelova, Durstewitz, & Yang, 2001; Trantham-Davidson, Neely, Lavin, & Seamans, 2004).

Both D1 and D2 dopamine receptors and the $GABA_A$ receptor are highly enriched in the *Drosophila* MB (Han et al., 1996; Hearn et al., 2002; Kim et al., 2003; Liu, Krause, & Davis, 2007). Recent studies began to identify the dopaminergic role on the cell physiology in insects. A subset of MB-innervating dopaminergic neurons gate the MB output by releasing dopamine in fruit flies, and dopamine applies an inhibition to MB neurons (Krashes et al., 2009). A dopamine D1-like receptor in *Drosophila* was found to mediate the suppression of cholinergic synaptic transmission through a non-cAMP/protein kinase A signaling pathway (Yuan & Lee, 2007). Furthermore, the K^+ channel in MB Kenyon cells was shown to be a target molecule of dopamine in crickets (Aoki, Kosakai, & Yoshino, 2008). It revealed that besides second-messenger pathways, ion channels and protein kinase C also interact with D1-like receptors, similar to that seen in vertebrates. Future studies are expected to measure electrophysiological responses of MB neurons in various dopamine concentrations to test our assumptions on dopamine modulation.

2.5. Task design for computer simulation experiments

The task is divided into two stages: training and decision-making. Each trial takes 2 s. Two color bars with $\Delta COG = 60°$ are used for training, which invoke a preferred response of two bumps centered at units $P_1 = P_{b0}$ and $P_2 = P_{g0}$ in the P-module, respectively (Fig. 3(B)). Subscripts 'b' and 'g' mark the blue and green colors, respectively. At the same time two units in the C-module are activated by the preferred color. To make the description clear below, the blue bar is assumed to be coupled with heat punishment, while facing the green one is safe. According to the model's hypothesis on the topographic application of US input, heat US is applied to unit group centered at P_{b0} in the D-module once the blue bar enters the attention window. The choice task is different from training in two respects. First, the heat US input is removed. Second, the network is presented with two bars with their colors exchanged and ΔCOG decreased compared with that used for training. As shown in Fig. 3(C), two bumps centered at $P_1 = P_g$ and $P_2 = P_b$ are activated during the choice period.

2.6. Definition of choice PI

Model performance is evaluated by choice PI in B- or M-module, which is defined as $PI^{Mo} = (t_2 - t_1)/T$. T is trial duration, and t_1 (or t_2) is the accumulative time for the bump centered at unit P_1 (or P_2) to win competition within the module Mo. Since two bumps encodes danger and safe bar respectively (see task design above), t_1 and t_2 is actually the time for the model to make a decision with a preference for color or position cue.

The winner is determined by comparing the activity intensity between two bumps, which is measured by averaging frequencies among the units involved. In our simulations, the bump center unit together with its nearest neighbor six units is included in the operation of frequency averaging. The frequency of the bump centered at unit P_1 (or P_2) is denoted as f_1 (or f_2). If $(f_1 - f_2) > 0.5$, bump 1 wins the competition at the moment. And bump 2 wins if $(f_2 - f_1) > 0.5$. Other situations, in which the difference between f_1 and f_2 is less than 0.5, are classified to a hesitating or non-choice state. Note that individual units' firing frequencies are normalized to the range [0, 1] in the model.

3. Results

3.1. No preference for any visual target before learning

Drosophila without prior training tracks any visual stimulus randomly, i.e., shows no preference. It is the basis or starting point of experimental paradigm design of operant conditioning in a flight simulator. The fact is used to rectify our network before learning.

Let us present a pair of color bars to the model to test its initial preference. As an example, a pair of bars evoking bumps separately centered at units $P_1 = P_g = 19$ and $P_2 = P_b = 59$ in P-module is used (top panel in Fig. 4). Persistent activities of two units in the C-module detect and encode green and blue colors, respectively (data not shown). Because of no memory-dependent biasing from the D-module, the binding module is purely controlled by the attention window. It is found in simulations that the choice PI of the B-module (PI^B) may be any value ranging from -1.0 to $+1.0$ if the trial is repeated, which seriously deviates from a no-preference standard. It is easy to understand: for a given short trial like $T = 2$ s a random shifting of the attention window does not necessarily lead to an equal or roughly equal attention time to two bars. To ensure a no-preference performance, only the shifting patterns of the attention spotlight inducing a PI^B close to 0 or less than 0.1 are selected for computer simulations below. This can be easily realized in programming by remembering the random seed of the qualified random patterns. An instance with $P_g = 19$ and $P_b = 59$ is shown in Fig. 4, in which the dynamics and average frequency of two bumps in the B-module are illustrated.

Changing the bar separation ΔCOG denoted by parameter Δ to different values and repeating the trial in the same way as above, we obtain a PI curve only including PI^B close to zero (dashed line in Fig. 5(A)). Starting from the no-preference model for any bar stimulus, we investigate below how the memory and dopamine affect decision-making.

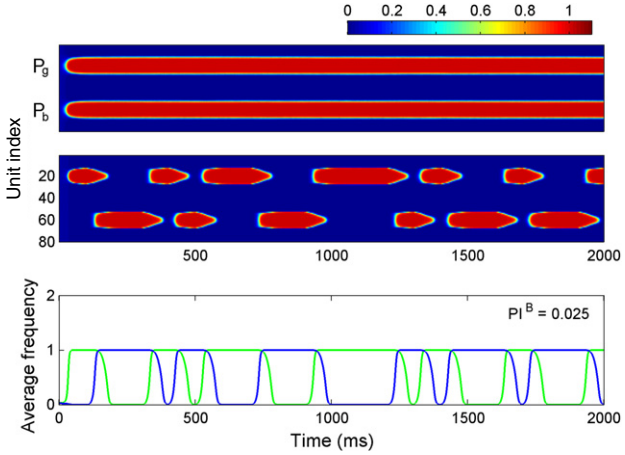

Fig. 4. Network dynamics before training. During a 2 s presentation of two bars with $P_g = 19$ and $P_b = 59$, unit activities within the P- and B-modules are respectively shown in the top and middle panel. Color indicates changes in normalized firing rate (see scale). The color scale also applies to Fig. 6(A), (C), and (D). The bottom panel gives the average frequencies of two bumps within the B-module with PI^B indicated.

3.2. Learning and feature-dependent memory

A 2 s-training trial is applied to the network, simulating the conditioning of *Drosophila* at the flight simulator. The M-module is excluded during this period, because MBs are dispensable for visual learning (Wolf et al., 1998). A pair of color bars with $\Delta COG = 60°$, $P_1 = P_{b0} = 10$, and $P_2 = P_{g0} = 70$ is used for visual stimuli, while an excitatory input US_i is given to a group of units i with $|i - P_{b0}| < 10$ in D-module, simulating the heat punishment as explained in Eq. (6). The simultaneous activation of two unit groups centered at $P_{b0} = 10$ in the P- and D-modules leads to synaptic plasticity. By using the learning rule in Eq. (7), specific connections $w_{ii}^{B\to D}$ from pre-synaptic units in the B-module to post-synaptic ones in the D-module are established during learning (Fig. 5(B)). Although the Oja rule is applied here, it does not mean that the training needs a unique learning rule. Computer simulations show that any Hebbian rule based on pre- and postsynaptic activity with synaptic weight normalization works (data not shown).

$w_{ii}^{B\to D}$ stores a kind of position-related memory. Because little is known about the color-dependent memory in *Drosophila*, it is not explicitly modeled in the study. A freely set function $f^C(\Delta)$ in Eq. (5) is simply used to simulate the inhibition effect on B-module of the conditioned color-related memory. The strength of $f^C(\Delta)$ is assumed to increase linearly when Δ approaches zero (Fig. 2(D)), while it is zero when Δ is greater than or equal to 30. $f^C(\Delta)$ simulates an increase in the relative saliency of the color cue with the decrease in the saliency of the position cue. Questions about the anatomic site of this color-dependent memory and the source of related inhibition still remain open.

3.3. Simple choice with defective or lesioned MB

The choice performance of a trained neural network in the task of Fig. 3(C) is tested without the M-module, mimicking the case in which flies with ablated MB structures or functions are confronted with conflicting cues. A decision is made in the B-module and can be fed directly to the motor center to initiate a behavior that is not part of the work. Facing a pair of bars with their colors exchanged compared with memory, the network is forced to decide which cue should be followed to avoid danger. Results show that the network weights the pros and cons naturally based on a feature-related memory. The closer the parameter P_g is to P_{b0}, the more salient the position cue is and the more

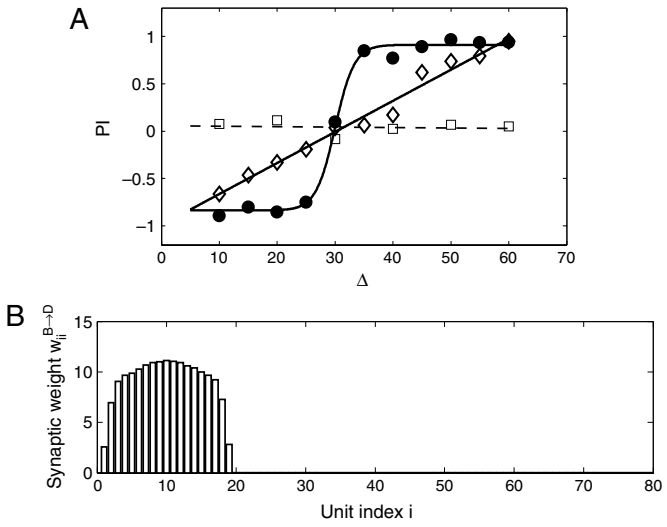

Fig. 5. (A) Choice curves for task in Fig. 3(C). Before the learning network shows no preference for two targets, which is evidenced by PI^B near zero (dashed line with square markers). After training, a linear choice behavior emerges in the circuit with the M-module excluded (solid line with diamond markers). In an intact network, the small choice PI originating from the B-module is substantially increased with dopamine modulation in the M-module, resulting in a clear-cut decision behavior (solid sigmoid curve with filled circle markers). Phasic dopamine begins from $t^r = 320$ ms and takes effect as $\alpha = 2.8$ and $\beta = 0.1$. (B) Feed-forward projections from the B- to D-modules. They are established during learning with learning rate $\tau^{\text{Learning}} = 40$ ms. The biggest synaptic weight occurs at $i = 10$.

strongly the D-module is activated through the learned synaptic weights $w_{ii}^{B\to D}$. The number of activated units in the D-module actually measures the extent of danger. An inhibitory feedback proportional to danger is projected from the D- to B-modules through hard connections $w_{ii}^{D\to B}$, weakening the bump centered at P_g. It makes the model tend to choose the bar encoded by the bump centered at P_b, resulting in a positive choice PI in the B-module PI^B. This is apparently a choice with preference for the position cue, and such a decision way dominates for $\Delta > 30$. Once $\Delta < 30$ is satisfied, the bump centered at P_b, to which the conditioned color is bound, is inhibited due to an increase of the color saliency as explained by the function $f^C(\Delta)$ in Eq. (5). Such an inhibition gradually becomes notable when Δ approaches zero (Fig. 2(D)), whereas the bump centered at P_g is relieved from the position memory-related inhibition. It results in another tendency for the model to make a decision with preference for the color cue, giving a negative PI^B.

In sum, the balance of no-preference for two bars before training is broken by memory-dependent biasing. Two bumps encoding potential choices are partially or completely inhibited depending on the relative saliency of position and color cues. To go deep into the choice process, three examples with $\Delta COG = \{50°, 40°, 15°\}$ are illustrated in Fig. 6 (with all M-module panels excluded). It can be seen that the D-module gradually loses excitation and becomes silent with the decrease of ΔCOG, highlighting an increase in the relative impact of the color cue on decision-making. By changing Δ and repeating the choice task, more data about the PI^B are obtained and fit well by a straight line, as shown by the solid line in Fig. 5(A). This linear choice curve accords with the behavioral data in Zhang et al. (2007).

3.4. Clear-cut decision-making with the involvement of dopamine-MB circuit

This section is devoted to probe how an intact network model makes decisions, given the choice task in Fig. 3(C). By 'intact', we mean the availability of both pathways in the model

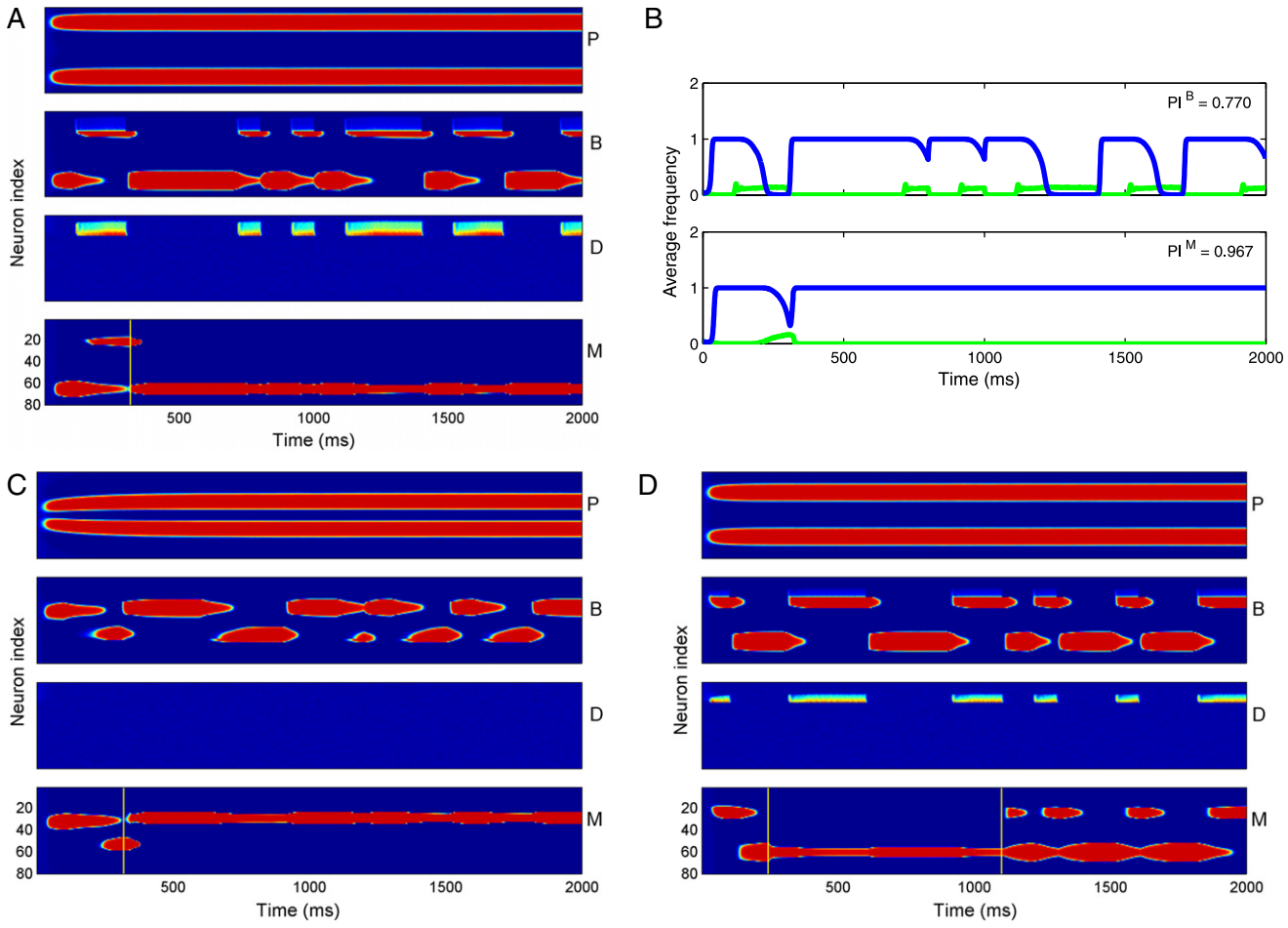

Fig. 6. Examples of choice process with different visual cues. (A) Unit activities during a choice trial with two bars described by $P_g = 14$ and $P_b = 64$. '*P*', '*B*', '*D*', and '*M*' on the right of each panel denote *P*-, *B*-, *D*-, and *M*-modules, respectively. Within the *M*-module the dopamine level is raised from $t^R = 320$ ms, which resets parameters $\alpha = 2.8$ and $\beta = 0.1$. (B) Average frequencies of two bumps of activity within the *B*- (top) and *M*-modules (bottom) in (A) with choice PIs indicated. (C) Choice process with $P_g = 32$ and $P_b = 47$. Other parameters are the same as that in A. Choice PIs are $\mathrm{PI}^B = -0.459$ and $\mathrm{PI}^M = -0.799$. (D) Choice process with $P_g = 19$ and $P_b = 59$. Dopamine level raising begins at 245 ms by setting parameter $\alpha = 5.0$ and ends at 1100 ms by resetting α back to the previous value as $\alpha = 1.0$. Yellow lines in *M*-module mark the onset time (A, C) or period of raised dopamine level (D).

(Fig. 1), simulating the case of wild-type flies. The second pathway via the MB is switched on by task complexity. The *M*-module receives direct projection from the *B*-module through hard synaptic connections. The choice PI in the *M*-module PI^M should be almost the same as PI^B if there is no other modulation. However, recognition of conflicting cues induces a phasic dopaminergic release to the *M*-module according to our model hypotheses. The onset time of dopamine increase is denoted by t^R, from which an increase of dopamine level critically promotes competition between two bumps by enhancing the lateral inhibition between units (Fig. 2(A)) and steepening the units' response function in the *M*-module (Fig. 2(C)). Two effects are separately simulated by an increase of parameter α in WI_{ij} and a decrease of parameter β in r_j^M. Fig. 6(A)–(C) give two examples with onset time $t^R = 320$ ms and raised dopamine level as $\alpha = 2.8$ and $\beta = 0.1$. Fig. 6(B) gives average frequencies of two bumps versus time during the choice process of the *B*- and *M*-modules in Fig. 6(A). Apparently the stronger bump completely soon wins the competition, resulting in a obviously improved choice PI^M compared with PI^B. This is clear-cut decision-making. To further investigate dopamine modulation, we first check the effect of parameters related with the dopamine level by fixing the onset time of an increase in dopamine release.

Take the task with $\Delta = 40$ ($P_g = 19$ and $P_b = 59$) as an instance. Set $t^R = 245$ ms, at which the stronger bump encoding the blue bar is dominating the *M*-module. To distinguish the roles of enhanced lateral inhibition and gain of unit response, only one of the single parameters α and β is changed in simulations. Results find that there exists a proper range of parameter α, in which the stronger bump soon completely wins the competition. As shown by the red curve in the left panel in Fig. 7, increasing α to any value within the range $\alpha \geq 4.0$, while keeping β unaffected by increased dopamine, results in a total win of the stronger bump. Such clear-cut choices are quantitatively indicated by a rise in $\mathrm{PI}^M - \mathrm{PI}^B$ from around 0.1 before raising dopamine to around 0.7. In contrast, our simulations show that enhancing the gain of unit response itself, simulated by a decreased β, does not work for getting a clear-cut choice (red curve in middle panel in Fig. 7), except that lateral inhibition is enhanced at the same time (black curve in middle panel in Fig. 7). Moreover, we find that simultaneously decreasing parameter β can extend the proper range of α required for a clear-cut choice to smaller values. For example, $\alpha \geq 2.5$ together with $\beta = 0.1$ is enough for a choice very similar to that reached by $\alpha \geq 4.0$ alone (black curve in left panel in Fig. 7).

To find out whether and how the onset time of dopamine increase affects the final choice, we repeat simulations as above except using different onset times. Results show that there exist proper dopamine levels that can ensure a total win of the stronger bump so long as the increased dopamine begins when the stronger bump either dominates the *M*-module or coexists with the weaker one. Otherwise, the weaker bump has a chance to be turned

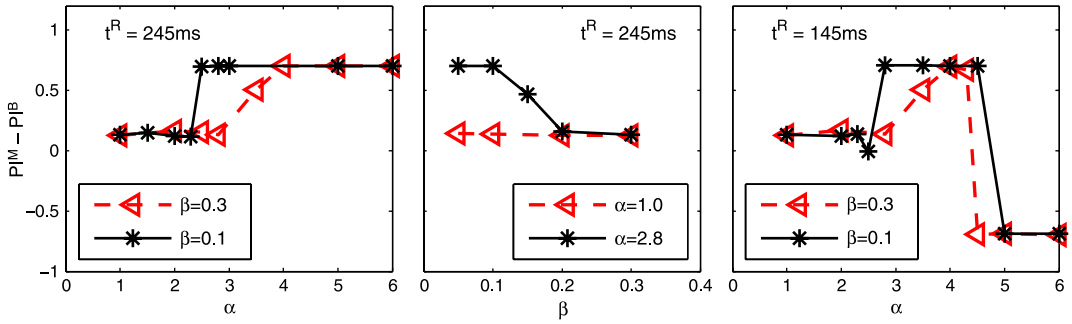

Fig. 7. Robustness of dopamine modulation against variations of single parameters α, β, and t^R. All choice trials have the same visual cues with $P_g = 19$ and $P_b = 59$. Decision-making behavior are quantified by choice PI difference $PI^M - PI^B$. See text for details.

into a winner if the enhanced lateral inhibition is large enough. Coexistence of two bumps happens around a transition of the attention window, during which competition is found to be more sensitive to a raised dopamine level. One example is $t^R = 145$ ms around the first attention transition. The optimal range of α required for the stronger bump to win the choice narrows (the right panel in Fig. 7) compared with the case with $t^R = 245$ ms (the left panel in Fig. 7). Much greater α even turns the weaker bump encoding the green bar into the winner, as shown by a negative $PI^M - PI^B$. It can be understood if we notice that enhanced lateral inhibition takes effect not only between bumps but also within single bumps. These simulations predict that increased dopamine concentration, should begin when the 'salient' bar enters the attention window. It should be at least after the attention window scans each target once, which is the minimal time to perceive visual stimuli.

It is interesting to note an inverted U-shape of optimal dopamine levels (the right panel in Fig. 7). Actually in mammals the inverted U-shape effect of dopamine has been earlier demonstrated: either insufficient or excessive dopamine concentration impairs cognitive functions (Seamans & Yang, 2004). Our model predicts that a moderate or intermediate concentration of increased dopamine is also required in nonlinear decision tasks in *Drosophila*.

A natural question is what happens if dopamine returns to the previous level or base-line. We perform simulations by restricting phasic dopamine release within a finite period. Results show that clear-cut choices induced by phasic dopamine are rapidly replaced by a linear choice once parameters α and β return to initial values. An example is shown in Fig. 6(D), where raising dopamine is limited between two yellow lines in the M-panel. A well-recovered dynamics emerges in the M-module after dopamine returns to its previous level, showing that the dopamine modulation effect is reversible. Reversible dopamine modulation is meaningful to *Drosophila*, whose neural system can prepare for coming choices in a changing environment.

More examples with other different ΔCOG are performed to check the qualitative dependence of dopamine modulation on parameters α, β, and t^R. Results show a good consistency. The choice behavior of the network is quantified by computing PI^M as a function of Δ. We obtain a sigmoid choice curve as shown in Fig. 5(A). Compared with the simple linear choice, the involvement of dopamine in M-module makes the slight difference between bumps, originated from the memory-dependent biasing in the B-module, rapidly enlarged. It turns a hesitation between two visual targets into a clear-cut decision, which accounts for the saliency-based decision-making in Zhang et al. (2007).

Finally, it should be pointed out our model does not exclude other possible synaptic/cellular/circuit mechanisms of dopamine modulation, given that they are evidenced to function in enlarging the slight difference in activity between two neuron groups encoding two potential choices. A recent modeling study proposed that phasic dopamine induces a bistability in striatal spiny neurons, which plays a critical role in saliency-selective gating of the working memory from basal ganglia to the prefrontal cortex (Gruber et al., 2006; Gruber, Solla, Surmeier, & Houk, 2003). Whether similar effects of dopamine occur in the MB and take part in producing nonlinear choice behavior remains open.

4. Discussion

4.1. Testable predictions

Our model study makes several predictions that can be tested experimentally. Ambiguous/conflicting visual cues should activate dopaminergic neurons projecting to the MB, evoking a phasic dopamine increase in the MB. More accurately, phasic dopamine should begin when the animal perceives a difference in value between two visual targets. This prediction can be indirectly tested at a behavioral level: the time it takes to make a decision should be inversely proportional to $|\Delta\text{COG} - 30^\circ|$ in the task of Fig. 3(C). The larger the parameter $|\Delta\text{COG} - 30^\circ|$, the more rapidly the animal recognizes a difference in value between two bars based on memory. Take the case with $\Delta\text{COG} \approx 30^\circ$ as an example, in which the activities of two bumps projected from the B-module are almost equal. Our model predicts that no phasic dopamine release would occur. Of course, there are always random fluctuations in background activity *in vivo*. It could break the balance between two ideal input bars with no saliency. Thus in the case of $\Delta\text{COG} \approx 30^\circ$, whether phasic dopamine release is induced to promote a clear-cut decision in practice depends on whether a saliency difference is actually perceived or not, we speculate.

Another direct prediction is that significantly increased activation of GABA receptors should be observed in the MB in company with a raised dopamine level. If the signal-to-noise ratio of MB neurons can be measured *in vivo*, it should also be increased according to our model's results. Finally optimal dopamine levels should show an inverted U-shape in decision-making behavior in *Drosophila*.

4.2. Comparison with related models on decision-making

To our knowledge, the model is the first one aiming at simulations of decision making in *Drosophila*. From the viewpoint of the basic computations involved in making a choice in mammals (Gold & Shadlen, 2007; Rangel et al., 2008; Sugrue et al., 2005), the model is an oversimplification. It ignores such issues as action selection and outcome evaluation. And working memory that is thought necessary in the decision-making in insects (Menzel, 2009) has not been considered in the model yet. However, in spite of its simplicity the model reveals, at a systems-level,

the neurocomputational mechanism underlying the experience-dependent formation of value, the role of dopamine in the transformation from a linear to nonlinear decision, and etc.

Compared with biologically inspired models (Cisek, 2006; Lo & Wang, 2006; Soltani, Lee, & Wang, 2006; Soltani & Wang, 2006; Usher & McClelland, 2001; Wang, 2002), our model adopts previous ideas: encoding choice alternatives by different unit groups and resolving decision-making by a winner-take-all process. It is basically consistent with value-based choice models by Soltani et al. (2006) and Soltani and Wang (2006) in the sense that the value difference between two alternatives can be specifically computed at or traced to synaptic strength. On the other hand, the model essentially differs from previous ones. It aims at understanding two distinct choice behaviors: linear and nonlinear or clear-cut. The former leads to a choice probability directly proportional to a linear subtraction of alternative intensities or values, while the latter involves a nonlinear amplification of the linear subtraction by dopamine. Both involve a common selection mechanism and are value-based, but only the nonlinear choice can be observed in wild-type fruit flies confronted with conflicting cues. By contrast, other models (Soltani et al., 2006; Soltani & Wang, 2006) do not distinguish two categories of choice behaviors. In their models, choice behavior, quantified by the probability of choosing one target, is declared to be well-fitted by a sigmoid function of the input difference between two alternatives. But according to their data, it seems that a linear regression fits behavioral data much better than a sigmoid curve does (see Fig. 7 in Soltani et al. (2006), Fig. 3 in Soltani and Wang (2006), and Fig. 1(c) in Kepecs et al. (2008)). We are supposing that only when an additional mechanism, for instance, similar to the dopamine modulation in the model, is applied to their network, a true sigmoid function of choice probability vs. the input difference can occur. Another difference from their models lies in the hypothesis about anatomical location of plastic synapses underlying value formation. Input synapses on to a decision circuit are endowed with a plasticity (Soltani et al., 2006; Soltani & Wang, 2006), while our model proposes a separate memory area or danger detecting area for learning. Besides, our model has other apparent differences from previous ones, ranging from model structure to choice task design. We omit a detailed list here.

Escaping to a safe place is imperative for flies confronted with cues predicting punishment danger. Clear-cut decision is therefore the best strategy in face of conflicting cues implying possible danger, we believe, although it may not be an optimal one in face of conflicting cues invoking appetitive memory. In contrast with flies experienced in aversive reinforcement, most other models discussed above are based on an animal's appetitive memory. This may be a reason why those models do not distinguish two choice behaviors.

Bayesian methods are successful for developing computational theories for perception and sensorimotor control in a world of sensory uncertainty, and humans are believed to behave as optimal Bayesian observers (Beck et al., 2008; Knill & Pouget, 2004; Körding & Wolpert, 2006). Although we agree that drosophila may also use Bayesian inference to avoid danger and search for food sources in daily life, the choice task in Fig. 3(C) is an exception. According to Bayes rule, a fly's belief in that observed conflicting cues (denoted as o) mean heat danger (denoted as s) should be a probability function characterized by $p(\mathrm{o}/\mathrm{s})p(\mathrm{s})/p(\mathrm{o})$. However, the fly was present in only one case with $\Delta = 60$ in previous training, as shown in Fig. 3(B). Such conditioning does not allow flies to integrate information over cue position and color. The prior probability $p(\mathrm{s})$ could not be learned through the limited experience. How much more likely the truth of danger s makes o, quantified by the ratio $p(\mathrm{o}/\mathrm{s})/p(\mathrm{o})$, is also unavailable. We therefore think Bayesian considerations are not helpful in this study.

4.3. Role of dopamine in visual learning in Drosophila

Midbrain dopaminergic neurons in mammals encode a prediction-error signal to guide reward-related learning, as described in various reinforcement learning models like actor-critic ones (Dayan & Abbott, 2001; Montague, King-Casas, & Cohen, 2006; Sutton & Barto, 1998). At the cellular level dopamine modulation is required in synaptic plasticity, for example, at the corticostriatal synapses (Reynolds, Hyland, & Wickens, 2001; Reynolds & Wickens, 2002).

Very little is known about whether there is a similar error signal guiding learning in insects. For olfactory learning in *Drosophila*, dopaminergic neurons convey aversive reinforcement, contrasting with their established role in mammals. Octopaminergic neuronal activities are only necessary for conveying rewarding US in appetitive learning (Keene & Waddell, 2005; Riemensperger et al., 2005; Schroll et al., 2006; Schwaerzel et al., 2003 but see Kim, Lee, & Han, 2007 for the critical role of D1 dopamine receptor in both aversive and appetitive conditioning). With respect to visual learning in insects the role of dopamine is unclear, although dopamine has been reported to mediate aversive visual conditioning in crickets by a pharmacological approach (Unoki, Matsumoto, & Mizunami, 2006). During visual operant conditioning, like in Zhang et al. (2007), it is even more difficult to detect the dynamics of dopaminergic neurons. This is why the dopamine effect is excluded from the learning rule in Eq. (7), which is in contrast to a dopamine- or reward-dependent learning rule in previous models (Soltani et al., 2006; Soltani & Wang, 2006). Note that this exclusion does not affect the final association between CS and US in the model. Future physiological tools and experiments in conjunction with powerful fly genetics are expected to provide insights into the role of dopamine in visual learning in *Drosophila*.

4.4. Attention and MB

Fixation or tracking behavior induced by visual targets at a flight simulator was referred to as visual selective attention in fruit flies (Heisenberg et al., 2001; van Swinderen, 2005; Wu et al., 2000). Our model strongly proposes that paying attention to a visual target is separated from a fixation behavior towards the target, at least in the case of being confronted with a choice task. In addition, it should be noted that feedback from the MB to other modules is not considered in the model for simplification. But at least the MB was shown to be involved in selective attention (Xi et al., 2008). Future studies, especially by electrophysiological tools in *Drosophila*, are expected to provide new lights on these questions.

Besides a mediator of olfactory learning (for review see Davis, 2005; Heisenberg, 2003; Roman & Davis, 2001), the MB is a prominent insect brain structure linked to sensory integration, motor control, and certain types of learning and memory. It is interesting to note a similarity in cognitive function between the MB and the prefrontal cortex. As a main target of dopaminergic projection, the prefrontal cortex is considerably regulated for optimal cognitive function (Seamans & Yang, 2004). Flies lacking MBs seem to have difficulties in stopping spontaneous walking even if it meets a water moat. The attention-like tracking behavior is impaired in flies with deficient MB (Xi et al., 2008). The explanation of these defects in visual cognition and motor control cannot detour the gating role of dopaminergic-MB circuit elucidated in the model, we believe.

4.5. Modeling approach in Drosophila study

In contrast to that mathematical models have widely been applied to reveal the circuit mechanism in many animals even including relatively simple ones like *C. elegans*, so far the modeling efforts

are quite lacking in *Drosophila* studies (Olsen & Wilson, 2008). It is mainly due to a still difficult monitoring of specific activities in *Drosophila* neurons by electrophysiological measurements. On the other hand, we do note that modeling studies have begun on the MB function in olfactory associative learning/memory, sparse encoding, and pattern recognition (Finelli, Haney, Bazhenov, Stopfer, & Sejnowski, 2008; Huerta & Nowotny, 2009; Huerta, Nowotny, Garcia-Sanchez, Abarbanel, & Rabinovich, 2004; Nowotny, Huerta, Abarbanel, & Rabinovich, 2005; Smith, Wessnitzer, & Webb, 2008). These models were inspired by recordings in insects with a bigger body size (for example, in locusts Cassenaer & Laurent, 2007; Perez-Orive et al., 2002). Recent progress in techniques, from accurately locating visual memory (Liu et al., 2006; Pan et al., 2009) to recording salience-modulated local field potentials (van Swinderen & Greenspan, 2003) in *Drosophila* is expected to convert *Drosophila* to one of the better organisms for computational neuroscience. Our model is such an attempt by organizing anatomical and behavioral data recently obtained, which aims at elucidating the decision mechanism in a neural system as simply as fruit flies.

Acknowledgements

We would like to thank Dr. Ke Zhang for helpful discussions. We also thank the reviewers for their constructive comments. This work was supported by National Science Foundation of China (grants 30770495, 30630028, 90820008, 30770511, and 30921064) and the Knowledge Innovation Engineering Project of Chinese Academy of Sciences (grants KSCX2-YW-R-39 and KSCX2-YW-R-247).

References

Aoki, K., Kosakai, K., & Yoshino, M. (2008). Monoaminergic modulation of the Na^+-activated K^+ channel in Kenyon cells isolated from the mushroom body of the cricket (Gryllus bimaculatus) brain. *Journal of Neurophysiology*, *100*, 1211–1222.

Beck, J. M., Ma, W. J., Kiani, R., Hanks, T., Churchland, A. K., Roitman, J., Shadlen, M. N., Latham, P. E., & Pouget, A. (2008). Probabilistic population codes for Bayesian decision making. *Neuron*, *60*, 1142–1152.

Brunel, N., & Wang, X. J. (2001). Effects of neuromodulation in a cortical network model of object working memory dominated by recurrent inhibition. *Journal of Computational Neuroscience*, *11*(1), 63–85.

Cassenaer, S., & Laurent, G. (2007). Hebbian STDP in mushroom bodies facilitates the synchronous flow of olfactory information in locusts. *Nature*, *448*, 709–713.

Cisek, P. (2006). Integrated neural processes for defining potential actions and deciding between them: a computational model. *Journal of Neuroscience*, *26*, 9761–9770.

Cohen, J. D., Braver, T. S., & Brown, J. W. (2002). Computational perspectives on dopamine function in prefrontal cortex. *Current Opinion in Neurobiology*, *12*, 223–229.

Davis, R. L. (2005). Olfactory memory formation in Drosophila: from molecular to systems neuroscience. *Annual Review of Neuroscience*, *28*, 275–302.

Dayan, P., & Abbott, L. A. (2001). *Theoretical neuroscience: computational and mathematical modeling of neural systems*. Cambridge, MA: MIT Press.

Dill, M., & Heisenberg, M. (1995). Visual pattern memory without shape recognition. *Philosophical Transactions of the Royal Society of London. Series B*, *349*(1328), 143–152.

Durstewitz, D., Seamans, J. K., & Sejnowski, T. J. (2000). Dopamine mediated stabilization of delay-period activity in a network model of prefrontal cortex. *Journal of Neurophysiology*, *83*(3), 1733–1750.

Egelhaaf, M. (1985). On the neuronal basis of figure-ground discrimination by relative motion in the visual system of the fly II: figure detection cells, a new class of visual interneurons. *Biological Cybernetics*, *52*, 195–209.

Ernst, R., & Heisenberg, M. (1999). The memory template in Drosophila pattern vision at the flight simulator. *Vision Research*, *39*, 3920–3933.

Finelli, L. A., Haney, S., Bazhenov, M., Stopfer, M., & Sejnowski, T. J. (2008). Synaptic learning rules and sparse coding in a model sensory system. *PLoS Computational Biology*, *4*(4), e1000062. doi:10.1371/journal.pcbi.1000062.

Fiorillo, C. D., Tobler, P. N., & Schultz, W. (2003). Discrete coding of reward probability and uncertainty by dopamine neurons. *Science*, *299*, 1898–1902.

Fuxe, K., Dahlström, A., Jonsson, G., Marcellino, D., Guescini, M., Dam, M., et al. (2009). The discovery of central monoamine neurons gave volume transmission to the wired brain. *Progress in Neurobiology*, doi:10.1016/j.pneurobio.2009.10.012.

Gao, S., Takemura, S. Y., Ting, C. Y., Huang, S., Lu, Z., Luan, H., et al. (2008). The neural substrate of spectral preference in Drosophila. *Neuron*, *60*, 328–342.

Gilbert, C., & Strausfeld, N. J. (1992). Small-field neurons associated with oculomotor and optomotor control in muscoid flies: functional organization. *Journal of Comparative Neurology*, *316*, 72–86.

Gorelova, N., Seamans, J. K., & Yang, C. R. (2002). Mechanisms of dopamine activation of fast-spiking interneurons that exert inhibition in rat prefrontal cortex. *Journal of Neurophysiology*, *88*, 3150–3166.

Gold, J. I., & Shadlen, M. N. (2007). The neural basis of decision making. *Annual Review of Neuroscience*, *30*, 535–574.

Gruber, A. J., Dayan, P., Gutkin, B. S., & Solla, S. A. (2006). Dopamine modulation in the basal ganglia locks the gate to working memory. *Journal of Computational Neuroscience*, *20*, 153–166.

Guo, A., Zhang, K., Peng, Y., & Xi, W. (2009). Heisenberg's roadmap guides our journey to the small cognitive world of Drosophila. *Journal of Neurogenetics*, *23*, 100–103.

Guo, A., Zhang, K., Peng, Y., & Xi, W. (2010). Research progress on Drosophila visual cognition in China. *Sci. China Life Sci.*, *53*, 374–384.

Gruber, A. J., Solla, S. A., Surmeier, D. J., & Houk, J. C. (2003). Modulation of striatal single units by expected rewards: a spiny neuron model displaying dopamine-induced bistability. *Journal of Neurophysiology*, *90*, 1095–1114.

Han, K. A., Millar, N. S., Grotewiel, M. S., & Davis, R. L. (1996). DAMB, a novel dopamine receptor expressed specifically in Drosophila mushroom bodies. *Neuron*, *16*, 1127–1135.

Hearn, M. G., Ren, Y., McBride, E. W., Reveillaud, I., Beinborn, M., & Kopin, A. S. (2002). Drosophila dopamine 2-like receptor: molecular characterization and identification of multiple alternatively spliced variants. *Proceedings of the National Academy of Sciences USA*, *99*, 14554–14559.

Heisenberg, M. (2003). Mushroom body memoir: from maps to models. *Nature Reviews Neuroscience*, *4*, 266–275.

Heisenberg, M., & Wolf, R. (1984). In V. Braitenberg (Ed.), *Studies of brain function*: *vol. 12. Vision in Drosophila: genetics of microbehavior*. Berlin: Springer-Verlag.

Heisenberg, M., Wolf, R., & Brembs, B. (2001). Flexibility in a single behavioral variable of Drosophila. *Learning & Memory*, *8*, 1–10.

Huerta, R., & Nowotny, T. (2009). Fast and robust learning by reinforcement signals: explorations in the insect brain. *Neural Computation*, *21*, 2123–2151.

Huerta, R., Nowotny, T., Garcia-Sanchez, M., Abarbanel, H. D. I., & Rabinovich, M. I. (2004). Learning classification in the olfactory system of insects. *Neural Computation*, *16*, 1601–1640.

Itti, L., & Koch, C. (2001). Computational modeling of visual attention. *Nature Reviews Neuroscience*, *2*, 194–203.

Joesch, M., Plett, J., Borst, A., & Reiff, D. F. (2008). Response properties of motion-sensitive visual interneurons in the lobula plate of Drosophila melanogaster. *Current Biology*, *18*, 368–374.

Keene, A. C., & Waddell, S. (2005). Drosophila memory: dopamine signals punishment? *Current Biology*, *15*, R932–R934.

Kepecs, A., Uchida, N., Zariwala, H. A., & Mainen, Z. F. (2008). Neural correlates, computation and behavioural impact of decision confidence. *Nature*, *455*, 227–231.

Kim, Y. C., Lee, H. G., & Han, K. A. (2007). D1 Dopamine receptor dDA1 is required in the mushroom body neurons for aversive and appetitive learning in Drosophila. *Journal of Neuroscience*, *27*, 7640–7647.

Kim, Y. C., Lee, H. G., Seong, C. S., & Han, K. A. (2003). Expression of a D1 dopamine receptor dDA1/DmDOP1 in the central nervous system of Drosophila melanogaster. *Gene Expression Patterns*, *3*, 237–245.

Knill, D. C., & Pouget, A. (2004). The Bayesian brain: the role of uncertainty in neural coding and computation. *Trends in Neurosciences*, *27*, 712–719.

Körding, K. P., & Wolpert, D. M. (2006). Bayesian decision theory in sensorimotor control. *Trends in Cognitive Sciences*, *10*, 319–326.

Krashes, M. J., DasGupta, S., Vreede, A., White, B., Armstrong, J. D., & Waddell, S. (2009). A neural circuit mechanism integrating motivational state with memory expression in Drosophila. *Cell*, *139*, 416–427.

Liu, X., Krause, W. C., & Davis, R. L. (2007). $GABA_A$ receptor RDL inhibits Drosophila olfactory associative learning. *Neuron*, *56*, 1090–1102.

Liu, G., Seiler, H., Wen, A., Zars, T., Ito, K., Wolf, R., et al. (2006). Distinct memory traces for two visual features in the Drosophila brain. *Nature*, *439*, 551–556.

Lo, C. C., & Wang, X.-J. (2006). Cortico-basal ganglia circuit mechanism for a decision threshold in reaction time tasks. *Nature Neuroscience*, *9*, 956–963.

Mao, Z., & Davis, R. L. (2009). Eight different types of dopaminergic neurons innervate the Drosophila mushroom body neuropil: anatomical and physiological heterogeneity. *Frontiers in Neural Circuits*, *3*, 5.

Menzel, R. (2009). Working memory in bees: also in flies? *Journal of Neurogenetics*, *23*, 92–99.

Montague, P. R., Hyman, S. E., & Cohen, J. D. (2004). Computational roles of dopamine in behavioural control. *Nature*, *431*, 760–767.

Montague, P. R., King-Casas, B., & Cohen, J. D. (2006). Imaging valuation models in human choice. *Annual Review of Neuroscience*, *29*, 417–448.

Nicola, S. M., Surmeier, D. J., & Malenka, R. C. (2000). Dopaminergic modulation of neuronal excitability in the striatum and nucleus accumbens. *Annual Review of Neuroscience*, *23*, 185–215.

Nitz, D. A., van Swinderen, B., Tononi, G., & Greenspan, R. J. (2002). Electrophysiological correlates of rest and activity in Drosophila melanogaster. *Current Biology*, *12*, 1934–1940.

Nordstrom, K., Barnett, P. D., & O'Carroll, D. C. (2006). Insect detection of small targets moving in visual clutter. *PLoS Biology*, *4*, e54.

Nowotny, T., Huerta, R., Abarbanel, H. D. I., & Rabinovich, M. I. (2005). Self-organization in the olfactory system: rapid odor recognition in insects. *Biological Cybernetics*, *93*, 436–446.

Olsen, S. R., & Wilson, R. (2008). Cracking neural circuits in a tiny brain: new approaches for understanding the neural circuitry of Drosophila. *Cell*, *31*, 512–520.

Pan, Y., Zhou, Y., Guo, C., Gong, H., Gong, Z., & Liu, L. (2009). Differential roles of the fan-shaped body and the ellipsoid body in Drosophila visual pattern memory. *Learning & Memory*, *16*, 289–295.

Perez-Orive, J., Mazor, O., Turner, G. C., Cassenaer, S., Wilson, R. I., & Laurent, G. (2002). Oscillations and sparsening of odor representations in the mushroom body. *Science*, *297*, 359–365.

Rangel, A., Camerer, C., & Montague, P. R. (2008). A framework for studying the neurobiology of value-based decision making. *Nature Reviews Neuroscience*, *9*, 545–556.

Redgrave, P., & Gurney, K. (2006). The short-latency dopamine signal: a role in discovering novel actions? *Nature Reviews Neuroscience*, *7*, 967–975.

Reynolds, J. N. J., Hyland, B. I., & Wickens, J. R. (2001). A cellular mechanism of reward-related learning. *Nature*, *413*, 67–70.

Reynolds, J. N. J., & Wickens, J. R. (2002). Dopamine-dependent plasticity of corticostriatal synapses. *Neural Networks*, *15*, 507–521.

Riemensperger, T., Voeller, T., Stock, P., Buchner, E., & Fiala, A. (2005). Punishment prediction by dopaminergic neurons in Drosophila. *Current Biology*, *15*, 1953–1960.

Roman, G., & Davis, R. L. (2001). Molecular biology and anatomy of Drosophila olfactory associative learning. *BioEssays*, *23*, 571–581.

Schroll, C., Riemensperger, T., Bucher, D., Ehmer, J., Voller, T., Erbguth, K., et al. (2006). Light induced activation of distinct modulatory neurons triggers appetitive or aversive learning in Drosophila larvae. *Current Biology*, *16*, 1741–1747.

Schultz, W. (2007). Multiple dopamine functions at different time courses. *Annual Review of Neuroscience*, *30*, 259–288.

Schwaerzel, M., Monastirioti, M., Scholz, H., Friggi-Grelin, F., Birman, S., & Heisenberg, M. (2003). Dopamine and octopamine differentiate between aversive and appetitive olfactory memories in Drosophila. *Journal of Neuroscience*, *23*, 10495–10502.

Seamans, J. K., Gorelova, N., Durstewitz, D., & Yang, C. R. (2001). Bidirectional dopamine modulation of GABAergic inhibition in prefrontal cortical pyramidal neurons. *Journal of Neuroscience*, *21*, 3628–3638.

Seamans, J. K., & Yang, C. R. (2004). The principal features and mechanisms of dopamine modulation in the prefrontal cortex. *Progress in Neurobiology*, *74*, 1–57.

Servan-Schreiber, D., Printz, H., & Cohen, J. D. (1990). A network model of catecholamine effects: gain, signal-to-noise ratio, and behavior. *Science*, *249*, 892–895.

Smith, D., Wessnitzer, J., & Webb, B. (2008). A model of associative learning in the mushroom body. *Biological Cybernetics*, *99*, 89–103. doi:10.1007/s00422-008-0241-1.

Soltani, A., & Wang, X.-J. (2006). A biophysically based neural model of matching law behavior: melioration by stochastic synapses. *Journal of Neuroscience*, *26*, 3731–3744.

Soltani, A., Lee, D., & Wang, X.-J. (2006). Neural mechanism for stochastic behavior during a competitive game. *Neural Networks*, *19*, 1075–1090.

Sugrue, L. P., Corrado, G. S., & Newsome, W. T. (2005). Choosing the greater of two goods: neural currencies for valuation and decision making. *Nature Reviews Neuroscience*, *6*, 363–375.

Sutton, R. S., & Barto, A. G. (1998). *Reinforcement learning: an introduction*. Cambridge, MA: MIT Press.

Tang, S., & Guo, A. (2001). A choice behavior of Drosophila facing contradictory visual cues. *Science*, *294*, 1543–1547.

Tang, S., Wolf, R., Xu, S., & Heisenberg, M. (2004). Visual pattern recognition in Drosophila is invariant for retinal position. *Science*, *305*, 1020–1022.

Trantham-Davidson, H., Neely, L. C., Lavin, A., & Seamans, J. K. (2004). Mechanisms underlying differential D1 versus D2 dopamine receptor regulation of inhibition in prefrontal cortex. *Journal of Neuroscience*, *24*, 10652–10659.

Treisman, A. (1998). Feature binding, attention and object perception. *Philosophical Transactions of the Royal Society of London. Series B*, *353*, 1295–1306.

Turner, G. C., Bazhenov, M., & Laurent, G. (2008). Olfactory representations by Drosophila mushroom body neurons. *Journal of Neuroscience*, *99*, 734–746.

Unoki, S., Matsumoto, Y., & Mizunami, M. (2006). Roles of octopaminergic and dopaminergic neurons in mediating rewards and punishment signals in insect visual learning. *European Journal of Neuroscience*, *24*, 2031–2038.

Usher, M., & McClelland, J. L. (2001). The time course of perceptual choice: the leaky, competing accumulator model. *Psychological Review*, *108*, 550–592.

van Swinderen, B. (2005). The remote roots of consciousness in fruit-fly selective attention? *BioEssays*, *27*, 321–330.

van Swinderen, B., & Greenspan, R. J. (2003). Salience modulates 20–30 Hz brain activity in Drosophila. *Nature Neuroscience*, *6*, 579–586.

Wang, X.-J. (2002). Probabilistic decision making by slow reverberation in cortical circuits. *Neuron*, *36*, 955–968.

Wolf, R., Wittig, T., Liu, L., Wustmann, G., Eyding, D., & Heisenberg, M. (1998). *Drosophila* mushroom bodies are dispensable for visual, tactile, and motor learning. *Learn. Mem.*, *5*, 166–178.

Wu, Z., Gong, Z., Feng, C., & Guo, A. (2000). An emergent mechanism of selective visual attention in Drosophila. *Biological Cybernetics*, *82*, 61–68.

Xi, W., Peng, Y., Guo, J., Ye, Y., Zhang, K., Yu, F., et al. (2008). Mushroom bodies modulate salience-based selective fixation behavior in Drosophila. *European Journal of Neuroscience*, *27*, 1441–1451.

Yang, C. H., Belawat, P., Hafen, E., Jan, L. Y., & Jan, Y. N. (2008). Drosophila egg-laying site selection as a system to study simple decision-making processes. *Science*, *319*, 1679–1683.

Yuan, N., & Lee, D. (2007). Suppression of excitatory cholinergic synaptic transmission by Drosophila dopamine D1-like receptors. *European Journal of Neuroscience*, *26*, 2417–2427.

Zhang, K., Guo, J., Peng, Y., Xi, W., & Guo, A. (2007). Dopamine-mushroom body circuit regulates saliency-based decision-making in Drosophila. *Science*, *316*, 1901–1904.